It's okay to be green: Draft genome of the North American Bullfrog (Rana [Lithobates] catesbeiana)

S. Austin Hammond[1], René L. Warren[1], Benjamin P. Vandervalk[1], Erdi Kucuk[1], Hamza Khan[1], Ewan A. Gibb[1], Pawan Pandoh[1], Heather Kirk[1], Yongjun Zhao[1], Martin Jones[1], Andrew J. Mungall[1], Robin Coope[1], Stephen Pleasance[1], Richard A. Moore[1], Robert A. Holt[1], Jessica M. Round[2], Sara Ohora[2], Nik Veldhoen[2], Caren C. Helbing[2], Inanc Birol[1].

[1] Canada's Michael Smith Genome Sciences Centre, BC Cancer Agency, Vancouver, BC, Canada;

[2] Department of Biochemistry and Microbiology, University of Victoria, Victoria, BC, Canada

Abstract

Frogs play important ecological roles as sentinels, insect control and food sources. Several species are important model organisms for scientific research to study embryogenesis, development, immune function, and endocrine signaling. The globally-distributed Ranidae (true frogs) are the largest frog family, and have substantial evolutionary distance from the model laboratory frogs *Xenopus tropicalis* and *Xenopus laevis.* Consequently, the extensive *Xenopus* genomic resources are of limited utility for Ranids and related frog species. More widely-applicable amphibian genomic data is

1

urgently needed as more than two-thirds of known species are currently threatened or are undergoing population declines.

Herein, we report on the first genome sequence of a Ranid species, an adult male North American bullfrog (*Rana* [*Lithobates*] *catesbeiana*). We assembled high-depth Illumina reads (88-fold coverage), into a 5.8 Gbp (NG50 = 57.7 kbp) draft genome using ABySS v1.9.0. The assembly was scaffolded with LINKS and RAILS using pseudo-long-reads from targeted *de novo* assembler Kollector and Illumina TruSeq, as well as reads from long fragment (MPET) libraries. We predicted over 22,000 protein-coding genes using the MAKER2 pipeline and identified the genomic loci of more than 6,000 candidate long noncoding RNAs (lncRNAs) from a composite reference bullfrog transcriptome. Mitochondrial sequence analysis supports the phylogenetic positioning of the bullfrog within the genus *Rana* rather than *Lithobates*. Our draft bullfrog genome will serve as a useful resource for the amphibian research community and we demonstrate its utility in RNA-seq experiments to identify differential gene expression in the back skin of premetamorphic tadpoles subjected to thyroid hormone treatment.

Introduction

Amphibians have an undeniable role as sentinel species, as food source, and in insect control, yet are subject to multiple threats to their survival. Diseases and infections such as chytrid fungus (Raffel, et al., 2013), iridovirus (Lesbarrères, et al., 2012), and trematode parasites (Hayes, et al., 2010) are causing local and regional die-offs. In tandem with habitat loss, which is exacerbated by climate change, these factors have resulted in a worldwide amphibian extinction event unprecedented in recorded history:

over two-thirds of ~7,000 extant species are currently threatened or declining in numbers (AmphibiaWeb, 2017).

Frogs are important keystone vertebrates and have provided key discoveries in the fields of ecology, evolution, biochemistry, physiology, endocrinology, and toxicology (Helbing, 2012). Few frog genomes are available, and none represent a member of the Ranidae (true frogs), the largest frog family with species found on every continent except Antarctica. The North American bullfrog, *Rana (Lithobates) catesbeiana*, is an ideal species for building a representative Ranid genomic resource because it is consistently diploid, and has the widest global distribution of any true frog. Originally from eastern North America, the bullfrog has been introduced throughout the rest of North America, South America, Europe and Asia. It is farmed for food in many locations worldwide, and is considered an invasive species in several regions (Liu and Li, 2009).

The genomes of two *Xenopus* species (*X. tropicalis* and *X. laevis*) have been sequenced and annotated to some extent (Buisine, et al., 2015; Session, et al., 2016), but these pipids have an estimated divergence from the Ranidae ~260 million years ago (Sumida, et al., 2004). This evolutionary separation is accentuated by their differing life histories, behavior, markedly different sex differentiation systems (Eggert, 2004); and recent evidence suggests that the innate immune system of Xenopus is fundamentally different from three frog families including the Ranidae (Kiemnec-Tyburczy, et al., 2012). As a consequence, the degree of sequence variation is such that *Xenopus* genomic and transcriptomic resources are inadequate for studying ranid species (Helbing, 2012). The genome of a more-closely related frog, the Tibetan Plateau frog (*Nanorana parkeri*), has been recently released (Sun, et al., 2015), though this species

is also substantially separated from Ranids by approximately 89 million years (http://timetree.org/).

Using some of the latest sequencing and bioinformatics technologies, we have sequenced, assembled, and annotated an initial draft sequence of the ~5.8 billion nucleotide North American bullfrog genome (NG50 length 57,718 bp). We predicted 52,751 transcripts from 42,387 genes, of which 22,204 had supported biological evidence and were deemed high confidence. We anticipate that this much needed resource, which we make public alongside comprehensive transcriptome assembly data, will provide a valuable resource that will not only directly and immediately impact genetic, epigenetic, and transcriptomic bullfrog studies, but will also be enabling for developmental biology research ranging from amphibians to mammals, provide direly needed insights to curb rapidly declining ranid populations, and further our understanding of frog evolution.

Methods

Sample collection

Liver tissue was collected from an adult male *R. catesbeiana* specimen that had been caught in Victoria, BC, Canada and housed at the University of Victoria Outdoor Aquatics Unit. The tissue was taken under the appropriate sanctioned protocols and permits approved by the University of Victoria Animal Care Committee (Protocol #2015-028) and British Columbia Ministry of Forests, Lands and Natural Resource Operations (MFLNRO) permit VI11-71459. This frog was euthanized using 1% w/v tricaine methane sulfonate in dechlorinated municipal water containing 25 mM sodium

bicarbonate prior to tissue collection. Dissected liver pieces were preserved in RNA*later* (Thermo Fisher Scientific Inc., Waltham, MA, USA) at room temperature followed by incubation at 4°C for 24 h. Tissue samples were subsequently moved to storage at -20°C prior to DNA isolation. Total DNA was isolated using the DNeasy Blood and Tissue Kit (QIAGEN Inc., Mississauga, ON, Canada; Cat# 69506) with the inclusion of RNase treatment as per the manufacturer's protocol and stored at -20 °C prior to library preparation.

DNA library preparation and sequencing

All reagent kits used were from the same vendor (Illumina, San Diego, CA) unless otherwise stated. Two sets of paired-end tag (PET) libraries were constructed: 1) sixteen libraries were produced using 1 μg of DNA using custom NEBNext DNA Library Prep Reagents from New England BioLabs Canada (Whitby, ON); and 2) four libraries were constructed using 0.5 μg of DNA and the custom NEB Paired-End Sample Prep Premix Kit (New England BioLabs Canada). DNA sequence reads were generated from these libraries according to the manufacturer's instructions on the Illumina HiSeq 2000 platform (Illumina, San Diego, CA) in "High Throughput" mode with the HiSeq SBS Kit v3, on the Illumina HiSeq 2500 platform in "Rapid" mode with the HiSeq Rapid SBS kit v1, or on the Illumina MiSeq platform with the MiSeq Reagent Kit v2. See Table 1 for additional details.

The mate pair (MPET, a.k.a. jumping) libraries were constructed using 4 μg of DNA and the Nextera Mate Pair Library Preparation Kit, according to the manufacturer's protocol. One-hundred bp paired-end reads were generated on the Illumina HiSeq 2000 platform with the HiSeq SBS Kit v3.

The Synthetic Long Read (SLR, a.k.a. Moleculo) library was constructed using 500 ng DNA and Illumina's TruSeq SLR library prep kit with 8 - 10 kb size DNA fragments. Libraries were loaded on an Illumina HiSeq 2500 platform for 125 bp paired end sequencing.

Combined, this approach accounted for 88-fold sequence coverage of the approximately 6 Gbp bullfrog genome (Table 1).

Computing hardware

Sequence assemblies were performed on high performance computer clusters located at the Canada's Michael Smith Genome Sciences Centre, and consisted of nodes with 48 GB of RAM and dual Intel Xeon X-5650 2.66GHz CPUs running Linux CentOS 5.4 or 128 GB RAM and dual Intel Xeon E5-2650 2.6 GHz CPUs running Linux CentOS 6. Computational analyses used either this hardware, or nodes consisting of 24 GB of RAM and dual Intel Xeon X-5550 2.67 GHz CPUs running Red Hat Enterprise Linux 5 as part of WestGrid, Compute Canada.

Read merging

PET read pairs were merged sequentially using the ABySS-mergepairs tool (Birol, et al., 2013) and Konnector (version 1.9.0) (Vandervalk, et al., 2015). Bloom filters were constructed from all reads using the ABySS-Bloom utility (Warren, et al., 2015) and every tenth value of k between 75 and 245 bp, inclusive. Reads from potentially mixed clusters on the sequencing flow cells (determined by the Illumina chastity flag) were discarded, and the remaining reads were trimmed to the first base above a quality threshold (Q=3 on the phred scale) prior to merging.

Assembly process

ABySS (version 1.9.0) was used to reconstruct the *R. catesbeiana* genome (Simpson, et al., 2009). For the initial sequence assembly, three sets of reads were used: (i) Merged reads described above from paired-end Illumina HiSeq 150 bp, 250 bp, and MiSeq 500 bp libraries, (ii) unmerged reads from these same libraries, and (iii) TruSeq Synthetic Long-Reads. The unmerged HiSeq and MiSeq PET reads were also used for paired linking information to generate contigs. Finally, the MPET reads were used to bridge over regions of repetitive sequence to form scaffolds (see Table 1 for summary statistics of the sequencing data).

A certain fraction of the unresolved bases within these scaffolds were recovered using Sealer version 1.9.0 (Paulino, et al., 2015). Sealer uses a Bloom filter representation of a de Bruijn graph constructed using k-mers derived from the genomic reads to find a path between the sequences flanking scaffold gaps, and fill in the consensus sequence. In comparison to the fixed k-mer length of the whole genome assembly method, it uses a range of k-mer lengths to reflect different choices of sensitivity and specificity in detecting read-to-read overlaps. The Bloom filters that were used during the read merging phase were reused, and default values used for all parameters except for "--flank-length=260" and "--max-paths=10".

The resulting ABySS scaffold assembly (k = 160) was re-scaffolded with RAILS version 0.1 (Warren, 2016) (ftp://ftp.bcgsc.ca/supplementary/RAILS -d 250 -i 0.99) using both Moleculo long reads and Kollector (Kucuk, et al., *submitted*) targeted gene reconstructions (TGA; Supplemental Table 1). In RAILS, long sequences are aligned against a draft assembly (BWA-MEM V0.7.13-r1126 (Li, 2013) -a -t16), and the

7

alignments are parsed and inspected, tracking the position and orientation of each in assembly draft sequences, satisfying minimum alignment requirements (at minimum 250 anchoring bases with 99% sequence identity or more used in this study). Sequence scaffolding is performed using the scaffolder algorithms from LINKS (Warren, et al., 2015b), modified to automatically fill gaps with the sequence that informed the merge. The resulting assembly was sequentially re-scaffolded with a composite reference transcriptome (Bullfrog Annotation Resource for the Transcriptome; BART, Supplemental Table 1 and Supplemental Methods) with ABySS-longseqdist v1.9.0 (l=50, S=1000-) (Warren, et al., 2015a). It was further re-scaffolded iteratively with LINKS (v1.7) using a variety of long sequence data (Supplemental Table 1) including Moleculo-TruSeq (10 iterations –d 1-10:1 kbp, -t 10-1:-1, -k 20), MPET (-k 20, -t 5, -d 7.1 kbp, -e 0.9) and other assembly draft data (Kollector targeted reconstructions and k128 WGA combined, 7 iterations –d 1-15:2.5 kbp, -t 20,10,5,5,4,4,4 k=20).

Automated gap closing in the assembled scaffolds was again performed by Sealer. Completeness of the assembly was evaluated by comparison to a set of ultra-conserved core eukaryotic genes (Parra, et al., 2009).

Protein coding gene prediction

The MAKER2 genome annotation pipeline (version 2.31.8) was used to predict genes in the draft *R. catesbeiana* genome (Holt and Yandell, 2011). This framework included RepeatMasker (Smit, et al., 2013) to mask repetitive sequence elements based on the core RepBase repeat library (Jurka, et al., 2005). Augustus (Stanke, et al., 2006), SNAP (Korf, 2004) and GeneMark (Ter-Hovhannisyan, et al., 2008) were also run within the MAKER2 pipeline to produce *ab initio* gene predictions. BLASTx

8

(Camacho, et al., 2009), BLASTn (Camacho, et al., 2009), and exonerate (Slater and Birney, 2005) alignments of human and amphibian Swiss-Prot protein sequences (retrieved 16 February 2016) (UniProt, 2015) and BART were combined with the gene predictions to yield the gene models. MAKER2 was first applied to an early version of the bullfrog genome assembly, and the resulting gene models used for retraining as described in (Cantarel, et al., 2008).

We refined MAKER2's predicted gene list further by identifying a high confidence set, better suited for downstream biological analyses. Three criteria were considered: 1) The predicted transcripts must have at least one splice site, and all putative splice sites must be confirmed by an alignment to external transcript evidence; 2) the coding DNA sequence (CDS) of each transcript must have a BLASTn alignment to a BART contig with at least 95% identity along 99% of its length; or 3) the protein sequence encoded by the CDS must have a BLASTp (Camacho, et al., 2009) alignment to a human or amphibian Swiss-Prot protein sequence with at least 50% identity along 90% of its length (Supplemental Figure 1). The final assembly of the North American bullfrog genome with annotated MAKER2 gene predictions is available at NCBI-Genbank under accession (LIAG00000000, BioProject PRJNA285814).

Functional annotation

The high confidence set of transcripts was annotated according to the best BLASTp alignment of each putative encoded protein to the Swiss-Prot database (UniProt, 2015), when available. There were two levels of confidence for the annotations, 1) the most robust were identified using GeneValidator, which compares protein coding gene predictions with similar database proteins (Dragan, et al., 2016), where those having a

score of 90 or greater were definitively identified as the Swiss-Prot sequence they aligned to; and 2) all other annotated transcripts were considered to encode "hypothetical" proteins similar to their best Swiss-Prot hit, provided that they aligned with at least 25% identity along 50% of their length.

lncRNA prediction

To complement the protein coding gene predictions, a computational pipeline was developed to identify putative lncRNAs in the *R. catesbeiana* composite reference transcriptome BART (see Supplemental Methods for details). As there is a paucity of conserved sequence features that may positively identify lncRNA transcripts, we instead took a subtractive approach and omitted transcripts that were predicted to have coding potential or had sequence similarity to known protein encoding transcripts, as has been advocated in previous studies (Etebari, et al., 2015; Tan, et al., 2013). See Supplemental Methods for additional details.

We then used CD-HIT-EST (Fu, et al., 2012) (v4.6.6, -c 0.99) to identify and remove contigs with significantly redundant sequence content. The remaining transcripts were then interrogated for the presence of a polyA tail and one of 16 polyadenylation signal hexamer motifs (see Supplemental Table 3). The contigs were aligned to the genome assembly using GMAP (v2016-05-01, -f samse, -t 20) (Wu and Watanabe, 2005), and instances where there was a 3' sequence mismatch due to a run of As, or a 5' mismatch due to a run of Ts (in cases where the strand specific sequencing failed, and a RNA molecule complementary to the actual transcript was sequenced) prompted a search for the presence of a hexamer motif within 50 bp upstream (relative to the direction of coding) of the putative transcript cleavage site. Contigs containing a polyA tail and a

hexamer motif were selected for further analysis. We are aware that not all lncRNA are polyadenylated. The polyA tail filter was put in place to reduce the proportion of spurious transcripts, retained introns and assembly artifacts.

Candidate lncRNA transcripts were aligned to the draft genome with GMAP (version 2015-12-31, -f 2, -n 2, --suboptimal-score=0, --min-trimmed-coverage=0.9, --min-identity=0.9) (Wu and Watanabe, 2005), and those that had at least 90% of their sequence identified across no more than two separate genomic scaffolds with 90% sequence identity were retained. Alignments where the exon arrangement was not collinear with the original contig sequence were omitted. Further evidence of conservation of lncRNA candidates among amphibian species was obtained using a comprehensive amphibian transcriptome shotgun assembly database as described in the Supplemental Methods and Supplemental Table 3. The putative lncRNA sequences are available at the BCGSC ftp (ftp://ftp.bcgsc.ca/supplementary/bullfrog).

Differential gene expression analysis

As an example of the utility of the draft genome assembly and high confidence gene predictions, RNA-Seq reads from six premetamorphic *R. catesbeiana* tadpoles exposed to 10 pmol/g body weight thyroid hormone (3,3',5-triiodo-L-thyronine; T3) or dilute sodium hydroxide vehicle control for 48 h were used to characterize the T3-induced gene expression program in the back skin (see Supplemental Methods and Supplemental Table 2). The 100 bp paired-end reads were aligned to the draft genome using STAR (version 2.4.1d, --alignIntronMin 30, --alignIntronMax 500000, --outFilterIntronMotifs RemoveNoncanonicalUnannotated, --outFilterMismatchNMax 10, --sjdbOverhang 100) (Dobin, et al., 2013), and read counts per transcript were quantified

using HTSeq (version 0.6.1, default settings) (Anders, et al., 2015). Differential expression in response to T3 treatment was assessed using the DESeq2 software package (version 1.10.1, alpha=0.05) (Love, et al., 2014), and significance was considered where the Benjamini – Hochberg adjusted p-value was less than 0.05. Transcripts with zero counts in all six samples were excluded from the analysis. qPCR analysis of transcripts is described in the Supplemental Methods.

Gene ontology (GO) and pathway analysis

Due to the particularly extensive biological information available for human proteins, a second round of BLASTp alignments were performed between the high confidence set of predicted proteins and the Swiss-Prot human proteins, using the same alignment thresholds noted above. The Uniprot accession IDs and log fold-changes of the differentially expressed genes were collected, input to the Ingenuity® Pathway Analysis tool (Qiagen Bioinformatics, Redwood City, CA), and its core analysis was run with default settings. The Database for Annotation, Visualization and Integrated Discovery (DAVID) v6.8 (Huang, et al., 2009) was also used with default settings to perform gene annotation enrichment analysis on the differentially expressed genes versus the background of all bullfrog genes with Uniprot annotations. The enriched annotations were visualized with ReviGO (Supek, et al., 2011) with default settings.

Iridovirus integration experiment

The FV3 ranavirus genome and associated protein coding DNA sequences were downloaded from NCBI (GenBank Accession NC_005946.1), and aligned to the assembly with GMAP version 2015-12-31 (Wu and Watanabe, 2005) using default settings.

Mitochondrial genome assembly and finishing

The Mitochondrial (Mt) genome sequence was identified integrally in our whole genome assembly. Rounds of scaffolding effectively brought unincorporated Mt contigs to the edge of the scaffold, and after inspection were removed by breaking the redundant scaffolds at N's. Multiple sequence alignments were done between our sequence, two NCBI references originating from China (GenBank accessions NC02296 and KF049927.1) and one from Japan (AB761267), using MUSCLE (Edgar, 2004) from the MEGA phylogenetic analysis package (Kumar, et al., 2016) using default values. These analyses indicated that the mitochondrial sequence reported herein is most similar to the Japanese sequence, but with some discrepancies in two repeat regions, namely the absence of a 161 bp sequence at coordinate 15,270 and a 12-bp insertion at coordinate 9,214 relative to AB761267. We resolved these misassemblies using the correct Japanese reference sequence for these regions as candidates for a targeted *de novo* assembly of Illumina paired-end 250 bp reads with TASR (Warren and Holt, 2011); v1.7 with -w 1 -i 1 -k 15 -m 20 -o 2 -r 0.7). TASR uses whole reads for assemblies, and mitigates misassemblies otherwise caused by breaking reads into k-mers. The resulting TASR contigs that captured the correct sequences were inserted into our assembly in the corresponding regions. Transfer RNA (tRNA) and protein coding genes were annotated by GMAP alignment of the gene sequences included in KF049927.1. The Mt genome assembly was submitted to NCBI GenBank under accession KX686108.

Phylogenetic analyses

Complete mitochondrial genome sequences of selected salamanders and frogs (Supplemental Table 5) were compared using the MEGA phylogenetic package (Kumar,

et al., 2016). In another set of phylogenies, we also compared the mitochondrial genes

CYB and 12S and 16S rRNA RNR1 and RNR2 of selected amphibian species

(Supplemental Table 6). For these analyses, we first generated multiple sequence

alignments of the genome or gene sequences described above using either MUSCLE

(Edgar, 2004) or clustalw (Chenna, et al., 2003) (v1.83 with gap opening and extension

penalty of 15 and 6.66 for both the pairwise and multiple alignment stages, DNA weight

matrix IUB with transition weight of 0.5), and used the resulting pairwise alignments as

input for MEGA7 (Kumar, et al., 2016). The evolutionary history was inferred by using

the Maximum Likelihood method based on the Tamura-Nei model (Tamura and Nei,

1993), where initial trees for the heuristic search are obtained by applying Neighbor-Join

and BioNJ algorithms to a matrix of pairwise distances estimated using the Maximum

Composite Likelihood approach, and then selecting the topology with superior log

likelihood value.

Comparative genome analysis using Bloom filters

The genomes of *N. parkeri* (version 2; http://dx.doi.org/10.5524/100132), *X. tropicalis* (version 9.0, downloaded from xenbase.org) and *R. catesbeiana* (the present study) were compared for their k-mer (k=25) contents using ABySS-Bloom, a utility designed to approximate sequence divergence between draft genomes (Warren, et al., 2015a).

Repetitive sequence element detection

The content of repetitive sequence elements in the draft genome assembly was evaluated with RepeatMasker (version 4.0.6) (Smit, et al., 2013) with default settings. The RepBase collection of repeat sequence elements was supplemented with novel

elements identified using RepeatModeler (version 1.0.8) (Smit and Hubley, 2008) with RMBlast (version 2.2.27+, http://www.repeatmasker.org/RMBlast.html) applied to the draft genome assembly with default settings.

Results

We sequenced, assembled, and annotated the genome of the North American bullfrog, *R. catesbeiana*; a globally-distributed member of the true frogs. The draft assembly of the *R. catesbeiana* genome consists of 5.8 Gbp of resolved sequence (Table 2). The majority of reads from the PET libraries were successfully merged (63-75%), yielding longer pseudo-reads (AVG +/- SD, 446 +/- 107). The success of the pre-assembly read merging allowed us to use a value of the assembly k parameter greater than our shortest PET read length, increasing our ability to resolve short repetitive sequences. Genome scaffolding with orthogonal data, which included the BART reference transcriptome and scaffolds assembled at a lower k value greatly improved the contiguity of the resulting assembly (Table 2). We assessed the improvement to the assembly after each round of scaffolding using the NG50 length metric and the number of complete and partial core eukaryotic genes (CEGs) using CEGMA, which reports a proxy metric for assembly completeness (Parra, et al., 2009). Using the TruSeq synthetic long reads and the Kollector (Kucuk, et al., *submitted*) targeted gene assembly, RAILS (Warren, 2016) merged over 56 thousand scaffolds; this permitted the recovery of an additional four partial CEGs, and raised the contiguity of the assembly to approximately 30 kbp (Supplemental Table 1). The most dramatic improvements to assembly contiguity and resolved CEGs were obtained using LINKS (Warren, et al., 2015b) and the MPET reads (NG50 increase of ~16 kbp and 10 additional complete

15

CEGs; Supplemental Table 1), followed by the combined Kollector TGA and the lower-k WGA (~ 8 kbp improvement to NG50 and 9 additional complete CEGs; Supplemental Table 1).

The automated gap closing tool Sealer (Paulino, et al., 2015) was used twice during the assembly process. First, prior to the rounds of rescaffolding to increase the amount of resolved sequence available to inform the scaffolding algorithms, and then post-rescaffolding to improve the sequence contiguity and content for the MAKER2 gene prediction pipeline (Holt and Yandell, 2011). Sealer closed 55,657 gaps and resolved nearly 9 Mbp of sequence in the initial scaffolds, and further resolved 20 Mbp of sequence in its second round, closing 61,422 additional gaps.

We identified more than 60% of the *R. catesbeiana* genome as putative interspersed repeats (Supplemental Table 7). The draft bullfrog genome includes 101 (40.7%) "complete" CEGMA genes, and 212 "complete or partial genes" (85.5%). Application of the MAKER2 genome annotation pipeline to the final draft assembly resulted in a set of 42,387 predicted genes and 52,751 transcripts. The criteria applied to identify the high confidence set of genes reduced the population by approximately half, to 22,204 genes and 25,796 transcripts (Supplemental Figure 1). Of this high confidence set, 15,122 predicted proteins encoded by 12,671 genes could be assigned a functional annotation based on significant similarity to a SwissProt entry. Furthermore, 680 proteins from 590 genes were identified as particularly robust predictions by GeneValidator (Dragan, et al., 2016) (score ≥ 90). This 'golden' set includes several members of the Homeobox (HOX), Forkhead box (FOX), and Sry-related HMG box (SOX) gene families, which are transcription factors involved in developmental regulation (Kamachi and Kondoh, 2013;

16

Mallo and Alonso, 2013; Schmidt, et al., 2013). Immune-related genes, including interleukins 8 and 10, interferon gamma, and Toll-like receptors 3 and 4 were also confidently annotated.

lncRNA

The discovery and analysis of lncRNAs represents a new frontier in molecular genetics, and is of major relevance to the biology behind the functional and largely unexplored component of the transcriptome. The low degree of lncRNA primary sequence conservation between organisms, and the lack of selective pressure to maintain ORF integrity or codon usage complicates traditional similarity based discovery methods (Quinn and Chang, 2016). The exclusive approach to lncRNA detection that we employed identified 6,227 candidate lncRNA sequences.

Differential expression

Characterization of the regulatory factors that mediate TH-dependent initiation of tissue specific gene expression programs during metamorphosis have been extensively studied in *X. laevis*, although this species experiences markedly different environmental conditions in its natural habitat than many ranids do, and employed supraphysiological levels of TH (Buckbinder et al. 1992; Wang et al. 1993). Our present analysis of the TH-induced metamorphic gene expression program in the back skin detected nearly 6,000 genes significantly differentially expressed upon T3 treatment (Figure 1) including those found previously through targeted qPCR (Supplemental Table 8). The most prominent "biological process" gene ontologies associated with the Swiss-Prot derived functional annotations are related to RNA/DNA processing, signal transduction (including hormone signaling), and functions related to cell growth and division (Supplemental Figure 3). A

17

selection of new transcripts related to RNA/DNA processing were evaluated using qPCR and found to show similar relative abundance as observed with the RNA-seq data (Supplemental Figure 4, Supplemental Table 8). The effect of T3 treatment was not limited to the predicted protein coding genes, as expression of 1,085 candidate lncRNAs was also significantly affected.

Non-iridovirus sequence in bullfrog

Significant similarity to a frog virus 3 (FV3) protein was noted for one of the gene annotations. FV3 is the type species of the Ranavirus genus, so we explored the possibility that a FV3-like viral genome had wholly or partially integrated into the bullfrog specimen that we sequenced. The whole-genome and transcript alignments showed limited similarity between a single bullfrog scaffold and two FV3 sequences that encode hypothetical proteins, FV3gorf5R and FV3gorf98R (not shown). The region of similarity was identified as part of a conserved US22 domain (not shown).

Phylogenetic analysis of amphibian mitochondrial gene and genomes

Frog taxonomy is subject of debate (Pauly, et al., 2009). To address the controversy, we performed a number of phylogenetic experiments comparing selected amphibian mitochondrion (Mt) genomes and Mt genes at the nucleotide level (Figure 2). As expected, we observe clear separation of salamanders and toads (genus *Bufo*) from other species as outgroups (Figure 2A and Supplemental Figures 5 - 8). We color-coded the *Lithobates* and *Rana* in yellow and blue re-classified by Frost et al (2006) to identify the relative genus positioning within the generated phylogenetic trees. At least at the genetic level, *Lithobates* group branches out of the *Rana* group, as opposed to forming a distinct clade such as what is observed for salamanders and toads.

18

Comparing specific frog Mt gene CYB, *Rana* and *Lithobates* often branch together indicative of the close genetic conservation of these species, but do not form independent clades, which suggests a high degree of sequence conservation instead of the divergence observed between distinct genera (Figure 2B and Supplemental Figure 5). Ribosomal RNA genes RNR1 and RNR2 show phylogenies similar to that of the entire Mt genome, this time with *Rana* branching out of the *Lithobates* clade (Figure 2C and 2D, and Supplemental Figures 7 and 8).

Comparative genomics

Estimates of the genomic sequence identity between of *N. parkeri*, *X. tropicalis* and *R. catesbeiana* were performed. We did this using Bloom filters (Bloom, 1970), probabilistic data structures with bit sets for each genome's kmers (k=25). In a previous study, this method was shown to provide concordant estimates of the genome sequence divergence of known model organisms (human and apes), and was applied to conifer genomes (Warren, et al., 2015a).

This method is designed to compare the k-mer spectra of any two genomes by computing the k-mer set bit intersections of their respective Bloom filters. It is assumed that differences between the genomes are independently distributed. We point out that this method does not factor size differences in the genomes, nor structural rearrangements; instead it reports on the commonality over short sequence stretches. The reliability of the method also comes into question for very divergent genomes, as common k-mers are rarer and precise values of sequence identity are not expected. As such, divergence figures are likely an underestimate of their true separation. As observed, *R. catesbeiana* shares higher sequence identity ($86.0 +/- 3.3 \times 10^{-4}$ %) with the

19

High Himalaya frog (*N. parkeri*) than to the more evolutionarily diverged *X. tropicalis* ($79.2 +/- 3.4 \times 10^{-4}$ %), which is estimated to have shared a common ancestor with bullfrog more than 200 MYA, more than twice as much (89 MYA) as between *N. parkeri* and *R. catesbeiana* (Table 3).

Discussion

Amphibians are the only group where most of its members exhibit a life cycle that includes distinct independent aquatic larval and terrestrial juvenile/adult phases. The transition between the larval and juvenile phases requires substantial or complete remodeling of the organism (metamorphosis) in anticipation of a terrestrial lifestyle. Thus, this places amphibians in a unique position for the assessment of toxicological effects in both aquatic and terrestrial environments. As a model for human and mammalian perinatal development, including the transition from the aquatic environment of the womb to the outside world, *R. catesbeiana* is a preferable model to the *Xenopus* species, because of similar physiological transformations. In contrast, *Xenopus* remain aquatic throughout life (Helbing, 2012).

Our sequence divergence analysis with the recently released *Xenopus* genome of a diploid species, *X. tropicalis* (version 9.0) highlights the the reason why pipids are generally unsuitable genome references for ranid species due to their considerable evolutionary divergence. Our present work is consistent with earlier estimates of over ~200 million years ago. The initial assembly of another Xenopus species'genome of the allotetraploid *X. laevis* inbred 'J' strain has just been published (Session, et al., 2016). The haploid genomes of these species are substantially smaller (1.7 and 3.1 Gbp, respectively) than the typical ranid genome (Gregory, 2017). Despite the difference in

relative sizes, the comparative number of predicted protein-encoding genes for *R. catesbeiana* (~22,000) are comparable (45,099 *X. laevis*; ~20,000 *X. tropicalis*) (Hellsten, et al., 2010; Session, et al., 2016). However, the sequence divergence at the nucleic acid level confirms the empirical challenges of using *Xenopus* genomes as scaffolds for RNA-seq experiments of ranids. Even the recently published *N. parkeri* genome (Sun, et al., 2015), is substantially separated from *R. catesbeiana* by nearly 90 million years of evolutionary time (timetree.org).

The taxonomic classification of ranid species is contentious and highly debated amongst scholars (Pauly, et al., 2009). This stems largely from the suggested reclassification of the genus *Rana* in favor of *Lithobates* a few years ago (Frost, et al., 2008). Our phylogenetic analyses based on comparisons at the nucleotide level of complete mitochondrial genomes and genes from selected salamanders, toads, and ranids does not offer a rationale for the proposed change. It instead supports a close relationship between species classified as *Lithobates*, which may be considered a subgenus within the *Rana* genus. This observation is consistent with the recent phylogenetic analysis by Yuan et al. 2016.

The molecular mechanisms of amphibian metamorphosis have been predominantly studied using *X. laevis* and *X. tropicalis*, likely in no small part because their amenability to captive breeding, which ensures a ready supply of research specimens (Parker, et al., 1947). However, *Xenopus* larvae are typically much smaller than those of *R. catesbeiana*, with the consequence that each individual animal yields a smaller quantity of tissue for analysis. Indeed, *R. catesbeiana* tadpoles are large enough that techniques such as the cultured tail fin (C-fin) assay are possible, where multiple tissue biopsies

are collected from an individual animal and cultured *ex vivo* in a variety of hormone or chemical conditions (Hammond, et al., 2013; Hinther, et al., 2011; Hinther, et al., 2010; Hinther, et al., 2012). With this assay design each animal is effectively exposed simultaneously and independently to every condition in the experiment, and the result of these different conditions can be evaluated within each individual animal using powerful repeated-measures statistics.

Analysis of thyroid hormone-induced changes in tadpole back skin gene expression revealed an unprecedented view of the activation of new gene expression programs as an integral part of the transition from larval to adult skin. It is notable that the vast majority of annotated transcripts functioned in RNA/DNA processing roles. The wave of new transcripts that results from TH treatment must be spliced, capped with 7-methylguanosine, and polyadenylated. As the level of circulating TH increases in the tadpole, expression of key cell cycle control genes changes to regulate the proliferation of skin cells, including cyclin C and cyclin B (Buchholz, et al., 2007; Skirrow, et al., 2008; Suzuki, et al., 2009). This is in contrast to thyroid hormone-induced remodeling of the liver tissue where these cellular processes were not as prominently represented (Birol, et al., 2015).

Current lncRNA databases are mostly populated with sequences that were derived from human and mouse (Bu, et al., 2012; Quek, et al., 2015; Volders, et al., 2015). Recent studies involving bovine (Billerey, et al., 2014; Huang, et al., 2012; Weikard, et al., 2013), chicken (Li, et al., 2012), pig (Zhao, et al., 2015), diamondback moth (Etebari, et al., 2015), and goat (Ren, et al., 2016) have further contributed in enriching animal lncRNA datasets. A few databases exploring interactions of lncRNAs with

proteins, RNAs, and viruses have also been developed, but mainly describing interactions in human (Zhang, et al., 2014).In addition to expanding the effectiveness of RNA-seq analyses through annotation of protein-encoding transcripts, the present study identified over 6,000 putative lncRNA candidates in the bullfrog. Despite being non-coding with relatively low level of sequence conservation, some lncRNAs contribute to structural organization, function, and evolution of genomes (Derrien, et al., 2012). Examples include classical lncRNAs, such as X-inactive specific transcript (XIST), HOX transcript antisense RNA (HOTAIR), telomerase RNA component (TERC), and many more with roles in imprinting genomic loci (Thakur, et al., 2004), transcription (Feng, et al., 2006), splicing (Yan, et al., 2005), translation (Wang, et al., 2005), nuclear factor trafficking (Willingham, et al., 2005), chromatin modification, shaping chromosome conformation, and allosterically regulating enzymatic activity (Ponting, et al., 2009; Rinn and Chang, 2012). These functional roles overlap with the major gene ontologies associated with the protein coding genes differentially expressed in the T3-treated back skin. As the candidate lncRNAs that we identified represented nearly 1 in 5 of the differentially expressed genes, this suggests an important role for lncRNA in the amphibian metamorphic gene expression program initiated by TH. Further experiments to elucidate their role in this context are ongoing.

The bullfrog genome is larger than those of *N. parkeri, X. laevis*, and *X. tropicalis*, in concordance with earlier predictions for many Ranid genomes (Buisine, et al., 2015; Mazin, 1980; Session, et al., 2016; Sun, et al., 2015). Unlike *X. laevis*, this does not appear to be due to an allotetraploidization event in the Ranid progenitor species (Wang, et al., 2000; Zhu and Wang, 2006). Another possibility for genome enlargement

23

is integration of foreign DNA, which can manifest as DNA sequence repeat elements. Many of these integrations are likely to be derived from ancestral integration of viral genomes into the host genome (Belyi, et al., 2010). The genomes of Group I linear viruses, such as herpesviruses and FV3, include integrases which enable integration of their genetic material into that of the host cell during replication (Rohozinski and Goorha, 1992). However, the limited alignment of a single putative FV3 US22 domain found in many animal DNA viruses and some vertebrates (Zhang, et al., 2011), does not support the inclusion of a ranavirus genome into our assembled bullfrog genome *per se*, but may point to previous irreversible integration of viral genetic material in the evolutionary history of the bullfrog.

Conclusion

The *R. catesbeiana* genome presented herein provides an unprecedented resource for *Ranidae*. For example, it will inform the design and/or interpretation of high throughput transcriptome sequencing (RNA-seq), chromatin immunoprecipitation sequencing (ChIP-seq), and proteomics experiments. We anticipate that this resource will be valuable for conservation efforts such as identifying host/pathogen interactions and to identify environmental impacts of climate change and pollution on the development and reproduction of ranid species worldwide.

Acknowledgements

References

AmphibiaWeb (2017) Worldwide Amphibian Declines: How big is the problem, what are the causes and what can be done? Available at: www.amphibiaweb.org. [accessed January 4].

Anders, S., Pyl, P.T. and Huber, W. (2015) HTSeq - a Python framework to work with high-throughput sequencing data, *Bioinformatics*, **31**, 166-169.

Beaudoing, E*., et al.* (2000) Patterns of variant polyadenylation signal usage in human genes, *Genome res*, **10**, 1001-1010.

Belyi, V.A., Levine, A.J. and Skalka, A.M. (2010) Unexpected inheritance: multiple integrations of ancient bornavirus and ebolavirus/marburgvirus sequences in vertebrate genomes, *PLoS pathogens*, **6**, e1001030.

Billerey, C*., et al.* (2014) Identification of large intergenic non-coding RNAs in bovine muscle using next-generation transcriptomic sequencing, *BMC genomics*, **15**, 499.

Birol, I*., et al.* (2015) *De novo* transcriptome assemblies of *Rana* (*Lithobates*) *catesbeiana* and *Xenopus laevis* tadpole livers for comparative genomics without reference genomes, *PloS one*, **10**, e0130720.

Birol, I*., et al.* (2013) Assembling the 20 Gb white spruce (*Picea glauca*) genome from whole-genome shotgun sequencing data, *Bioinformatics*, **29**, 1492-1497.

Bloom, B.H. (1970) Space/time trade-offs in hash coding with allowable errors, *Commun Acm*, **13**, 422-426.

Bu, D*., et al.* (2012) NONCODE v3.0: integrative annotation of long noncoding RNAs, *Nucleic acids res*, **40**, D210-215.

Buchholz, D.R., *et al.* (2007) Pairing morphology with gene expression in thyroid hormone-induced intestinal remodeling and identification of a core set of TH-induced genes across tadpole tissues, *Dev biol*, **303**, 576-590.

Buisine, N., *et al.* (2015) *Xenopus tropicalis* genome re-scaffolding and re-annotation reach the resolution required for *in vivo* ChIA-PET analysis, *PloS one*, **10**, e0137526.

Camacho, C., *et al.* (2009) BLAST+: architecture and applications, *BMC bioinformatics*, **10**, 421.

Cantarel, B.L., *et al.* (2008) MAKER: an easy-to-use annotation pipeline designed for emerging model organism genomes, *Genome res*, **18**, 188-196.

Chenna, R., *et al.* (2003) Multiple sequence alignment with the Clustal series of programs, *Nucleic acids res*, **31**, 3497-3500.

Clark, K., *et al.* (2016) GenBank, *Nucleic acids res*, **44**, D67-72.

Derrien, T., *et al.* (2012) The GENCODE v7 catalog of human long noncoding RNAs: analysis of their gene structure, evolution, and expression, *Genome res*, **22**, 1775-1789.

Dobin, A., *et al.* (2013) STAR: ultrafast universal RNA-seq aligner, *Bioinformatics*, **29**, 15-21.

Dragan, M.A., *et al.* (2016) GeneValidator: identify problems with protein-coding gene predictions, *Bioinformatics*, **32**, 1559-1561.

Edgar, R.C. (2004) MUSCLE: multiple sequence alignment with high accuracy and high throughput, *Nucleic acids res*, **32**, 1792-1797.

Eggert, C. (2004) Sex determination: the amphibian models, *Reprod nutr dev*, **44**, 539-549.

Etebari, K., Furlong, M.J. and Asgari, S. (2015) Genome wide discovery of long intergenic non-coding RNAs in Diamondback moth (*Plutella xylostella*) and their expression in insecticide resistant strains, *Sci rep*, **5**, 14642.

Feng, J.*, et al.* (2006) The Evf-2 noncoding RNA is transcribed from the Dlx-5/6 ultraconserved region and functions as a Dlx-2 transcriptional coactivator, *Genes dev*, **20**, 1470-1484.

Finn, R.D.*, et al.* (2014) Pfam: the protein families database, *Nucleic acids res*, **42**, D222-230.

Finn, R.D.*, et al.* (2015) HMMER web server: 2015 update, *Nucleic acids res*, **43**, W30-38.

Frost, D.R.*, et al.* (2006) The amphibian tree of life, *Bull Am Mus Nat Hist*, **297**, 1-370.

Fu, L.*, et al.* (2012) CD-HIT: accelerated for clustering the next-generation sequencing data, *Bioinformatics*, **28**, 3150-3152.

Gregory, T.R. (2017) Animal Genome Size Database. Available at: www.genomesize.com. [accessed January 4].

Hammond, S.A., Carew, A.C. and Helbing, C.C. (2013) Evaluation of the effects of titanium dioxide nanoparticles on cultured *Rana catesbeiana* tailfin tissue, *Front genet*, **4**, 251.

Hammond, S.A., Veldhoen, N. and Helbing, C.C. (2015) Influence of temperature on thyroid hormone signaling and endocrine disruptor action in *Rana* (*Lithobates*) *catesbeiana* tadpoles, *Gen comp endocrinol*, **219**, 6-15.

Hayes, T.B*., et al.* (2010) The cause of global amphibian declines: a developmental endocrinologist's perspective, *The Journal of experimental biology*, **213**, 921-933.

Helbing, C.C. (2012) The metamorphosis of amphibian toxicogenomics, *Front genet*, **3**, 37.

Hellsten, U*., et al.* (2010) The genome of the Western clawed frog *Xenopus tropicalis*, *Science*, **328**, 633-636.

Hinther, A*., et al.* (2011) Effects of triclocarban, triclosan, and methyl triclosan on thyroid hormone action and stress in frog and mammalian culture systems, *Environ sci technol*, **45**, 5395-5402.

Hinther, A*., et al.* (2010) C-fin: a cultured frog tadpole tail fin biopsy approach for detection of thyroid hormone-disrupting chemicals, *Environ toxicol chem*, **29**, 380-388.

Hinther, A*., et al.* (2012) Influence of nitrate and nitrite on thyroid hormone responsive and stress-associated gene expression in cultured *Rana catesbeiana* tadpole tail fin tissue, *Front genet*, **3**, 51.

Holt, C. and Yandell, M. (2011) MAKER2: an annotation pipeline and genome-database management tool for second-generation genome projects, *BMC bioinformatics*, **12**, 491.

Huang, D.W., Sherman, B.T. and Lempicki, R.A. (2009) Systematic and integrative analysis of large gene lists using DAVID bioinformatics resources, *Nat protoc*, **4**, 44-57.

Huang, W., Long, N. and Khatib, H. (2012) Genome-wide identification and initial characterization of bovine long non-coding RNAs from EST data, *Anim genet*, **43**, 674-682.

Jurka, J*., et al.* (2005) Repbase Update, a database of eukaryotic repetitive elements, *Cytogenet genome res*, **110**, 462-467.

Kamachi, Y. and Kondoh, H. (2013) Sox proteins: regulators of cell fate specification and differentiation, *Development*, **140**, 4129-4144.

Kent, W.J. (2002) BLAT--the BLAST-like alignment tool, *Genome res*, **12**, 656-664.

Kiemnec-Tyburczy, K.M*., et al.* (2012) Genetic diversity of MHC class I loci in six non-model frogs is shaped by positive selection and gene duplication, *Heredity*, **109**, 146-155.

Kong, L*., et al.* (2007) CPC: assess the protein-coding potential of transcripts using sequence features and support vector machine, *Nucleic acids res*, **35**, W345-349.

Korf, I. (2004) Gene finding in novel genomes, *BMC bioinformatics*, **5**, 59.

Kucuk, E*., et al.* Kollector: transcript-informed, targeted *de novo* assembly of gene loci, *Bioinformatics* [submitted].

Kumar, S., Stecher, G. and Tamura, K. (2016) MEGA7: molecular evolutionary genetics analysis version 7.0 for bigger datasets, *Mol biol evol*, **33**, 1870-1874.

Lesbarrères, D*., et al.* (2012) Ranavirus: past, present and future, *Biol Letters*, **8**, 481-483.

Li, H. (2013) Aligning sequence reads, clone sequences and assembly contigs with BWA-MEM, arXiv:1303.3997v1301 [q-bio.GN].

Li, T.*, et al.* (2012) Identification of long non-protein coding RNAs in chicken skeletal muscle using next generation sequencing, *Genomics*, **99**, 292-298.

Liu, X. and Li, Y. (2009) Aquaculture enclosures relate to the establishment of feral populations of introduced species, *PloS one*, **4**, e6199.

Love, M.I., Huber, W. and Anders, S. (2014) Moderated estimation of fold change and dispersion for RNA-seq data with DESeq2, *Genome biol*, **15**, 550.

Maher, S.K.*, et al.* (2016) Rethinking the biological relationships of the thyroid hormones, l-thyroxine and 3,5,3'-triiodothyronine, *Comp biochem physiol D*, **18**, 44-53.

Mallo, M. and Alonso, C.R. (2013) The regulation of Hox gene expression during animal development, *Development*, **140**, 3951-3963.

Mazin, A.L. (1980) Amounts of nuclear-DNA in anurans of the USSR, *Experientia*, **36**, 190-191.

Parker, F.J., Robbins, S.L. and Loveridge, A. (1947) Breeding, rearing and care of the South African clawed frog (*Xenopus laevis*), *Am Nat*, **81**, 38-49.

Parra, G.*, et al.* (2009) Assessing the gene space in draft genomes, *Nucleic acids res*, **37**, 289-297.

Paulino, D.*, et al.* (2015) Sealer: a scalable gap-closing application for finishing draft genomes, *BMC bioinformatics*, **16**, 230.

Pauly, G.B., Hillis, D.M. and Cannatella, D.C. (2009) Taxonomic freedom and the role of official lists of species names, *Herpetologica*, **65**, 115-128.

Ponting, C.P., Oliver, P.L. and Reik, W. (2009) Evolution and functions of long noncoding RNAs, *Cell*, **136**, 629-641.

Quek, X.C.*, et al.* (2015) lncRNAdb v2.0: expanding the reference database for functional long noncoding RNAs, *Nucleic acids res*, **43**, D168-173.

Quinn, J.J. and Chang, H.Y. (2016) Unique features of long non-coding RNA biogenesis and function, *Nat rev genet*, **17**, 47-62.

Raffel, T.R.*, et al.* (2013) Disease and thermal acclimation in a more variable and unpredictable climate, *Nat clim change*, **3**, 146-151.

Ren, H.*, et al.* (2016) Genome-wide analysis of long non-coding RNAs at early stage of skin pigmentation in goats (Capra hircus), *BMC genomics*, **17**, 67.

Rinn, J.L. and Chang, H.Y. (2012) Genome regulation by long noncoding RNAs, *Ann revf biochem*, **81**, 145-166.

Robertson, G.*, et al.* (2010) *De novo* assembly and analysis of RNA-seq data, *Nat methods*, **7**, 909-912.

Rohozinski, J. and Goorha, R. (1992) A frog virus 3 gene codes for a protein containing the motif characteristic of the INT family of integrases, *Virology*, **186**, 693-700.

Schmidt, J., Piekarski, N. and Olsson, L. (2013) Cranial muscles in amphibians: development, novelties and the role of cranial neural crest cells, *J anat*, **222**, 134-146.

Session, A.M.*, et al.* (2016) Genome evolution in the allotetraploid frog *Xenopus laevis*, *Nature*, **538**, 336-343.

Simpson, J.T.*, et al.* (2009) ABySS: a parallel assembler for short read sequence data, *Genome res*, **19**, 1117-1123.

Skirrow, R.C.*, et al.* (2008) Roscovitine inhibits thyroid hormone-induced tail regression of the frog tadpole and reveals a role for cyclin C/Cdk8 in the establishment of the metamorphic gene expression program, *Dev dyn*, **237**, 3787-3797.

Slater, G.S. and Birney, E. (2005) Automated generation of heuristics for biological sequence comparison, *BMC bioinformatics*, **6**, 31.

Smit, A.F.A. and Hubley, R. (2008) RepeatModeler Open-1.0.

Smit, A.F.A., Hubley, R. and Green, P. (2013) RepeatMasker Open-4.0.

Stanke, M.*, et al.* (2006) Gene prediction in eukaryotes with a generalized hidden Markov model that uses hints from external sources, *BMC bioinformatics*, **7**, 62.

Sumida, M., Kato, Y. and Kurabayashi, A. (2004) Sequencing and analysis of the internal transcribed spacers (ITSs) and coding regions in the EcoR I fragment of the ribosomal DNA of the Japanese pond frog *Rana nigromaculata*, *Genes genet sys*, **79**, 105-118.

Sun, Y.B.*, et al.* (2015) Whole-genome sequence of the Tibetan frog *Nanorana parkeri* and the comparative evolution of tetrapod genomes, *Proc Natl Acad Sci U S A*, **112**, E1257-1262.

Supek, F.*, et al.* (2011) REVIGO summarizes and visualizes long lists of gene ontology terms, *PloS one*, **6**, e21800.

Suzek, B.E.*, et al.* (2015) UniRef clusters: a comprehensive and scalable alternative for improving sequence similarity searches, *Bioinformatics*, **31**, 926-932.

Suzuki, K.*, et al.* (2009) Molecular features of thyroid hormone-regulated skin remodeling in *Xenopus laevis* during metamorphosis, *Dev growth differ*, **51**, 411-427.

Tamura, K. and Nei, M. (1993) Estimation of the number of nucleotide substitutions in the control region of mitochondrial DNA in humans and chimpanzees, *Mol biol evol*, **10**, 512-526.

Tan, M.H.*, et al.* (2013) RNA sequencing reveals a diverse and dynamic repertoire of the *Xenopus tropicalis* transcriptome over development, *Genome res*, **23**, 201-216.

Ter-Hovhannisyan, V.*, et al.* (2008) Gene prediction in novel fungal genomes using an *ab initio* algorithm with unsupervised training, *Genome res*, **18**, 1979-1990.

Thakur, N.*, et al.* (2004) An antisense RNA regulates the bidirectional silencing property of the Kcnq1 imprinting control region, *Mol cell biol*, **24**, 7855-7862.

UniProt, C. (2015) UniProt: a hub for protein information, *Nucleic acids res*, **43**, D204-212.

Vandervalk, B.P.*, et al.* (2015) Konnector v2.0: pseudo-long reads from paired-end sequencing data, *BMC med genomics*, **8 Suppl 3**, S1.

Volders, P.J.*, et al.* (2015) An update on LNCipedia: a database for annotated human lncRNA sequences, *Nucleic acids res*, **43**, D174-180.

Wang, H.*, et al.* (2005) Dendritic BC1 RNA in translational control mechanisms, *J cell biol*, **171**, 811-821.

Wang, Y.J.*, et al.* (2000) High resolution late replication banding pattern of chromosomes in *Rana catesbeiana*, *Acta Zool Sinica*, **46**, 115-119.

Warren, R.L. (2016) RAILS and Cobbler: Scaffolding and automated finishing of draft genomes using long DNA sequences, *The Journal of Open Source Software*.

Warren, R.L. and Holt, R.A. (2011) Targeted assembly of short sequence reads, *PloS one*, **6**, e19816.

Warren, R.L.*, et al.* (2015a) Improved white spruce (*Picea glauca*) genome assemblies and annotation of large gene families of conifer terpenoid and phenolic defense metabolism, *Plant j*, **83**, 189-212.

Warren, R.L.*, et al.* (2015b) LINKS: Scalable, alignment-free scaffolding of draft genomes with long reads, *GigaScience*, **4**, 35.

Weikard, R., Hadlich, F. and Kuehn, C. (2013) Identification of novel transcripts and noncoding RNAs in bovine skin by deep next generation sequencing, *BMC genomics*, **14**, 789.

Willingham, A.T.*, et al.* (2005) A strategy for probing the function of noncoding RNAs finds a repressor of NFAT, *Science*, **309**, 1570-1573.

Wu, T.D. and Watanabe, C.K. (2005) GMAP: a genomic mapping and alignment program for mRNA and EST sequences, *Bioinformatics*, **21**, 1859-1875.

Yan, M.D.*, et al.* (2005) Identification and characterization of a novel gene Saf transcribed from the opposite strand of Fas, *Human molec genet*, **14**, 1465-1474.

Yuan, Z.Y.*, et al.* (2016) Spatiotemporal diversification of the True Frogs (Genus Rana): A historical framework for a widely studied group of model organisms, *Syst biol*, **65**, 824-842.

Zhang, D., Iyer, L.M. and Aravind, L. (2011) A novel immunity system for bacterial nucleic acid degrading toxins and its recruitment in various eukaryotic and DNA viral systems, *Nucleic acids res*, **39**, 4532-4552.

Zhang, X.*, et al.* (2014) RAID: a comprehensive resource for human RNA-associated (RNA-RNA/RNA-protein) interaction, *RNA*, **20**, 989-993.

Zhao, W., *et al.* (2015) Systematic identification and characterization of long intergenic non-coding RNAs in fetal porcine skeletal muscle development, *Sci rep*, **5**, 8957.

Zhu, C.B. and Wang, Y. (2006) A study on the chromosomes in bullfrog *Rana catesbeiana*, *Acta Laser Biol Sinica*, **15**, 305-307.
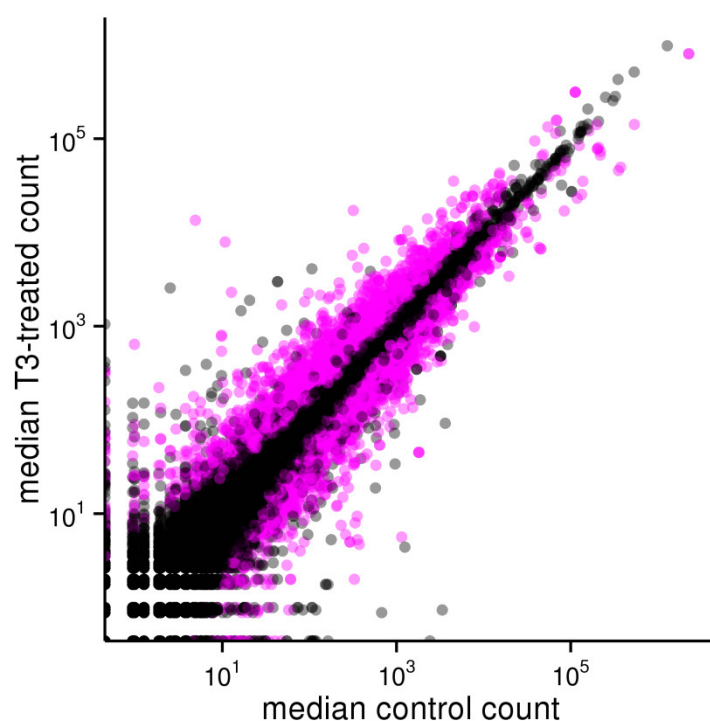
Figures

Figure 1. **Median counts of genes detected in the back skin of premetamorphic *R. catesbeiana* tadpoles treated with vehicle control or T3 for 48h**. Gene transcripts determined to be significantly differentially expressed (DESeq2 adjusted p-value < 0.05) are indicated in pink.
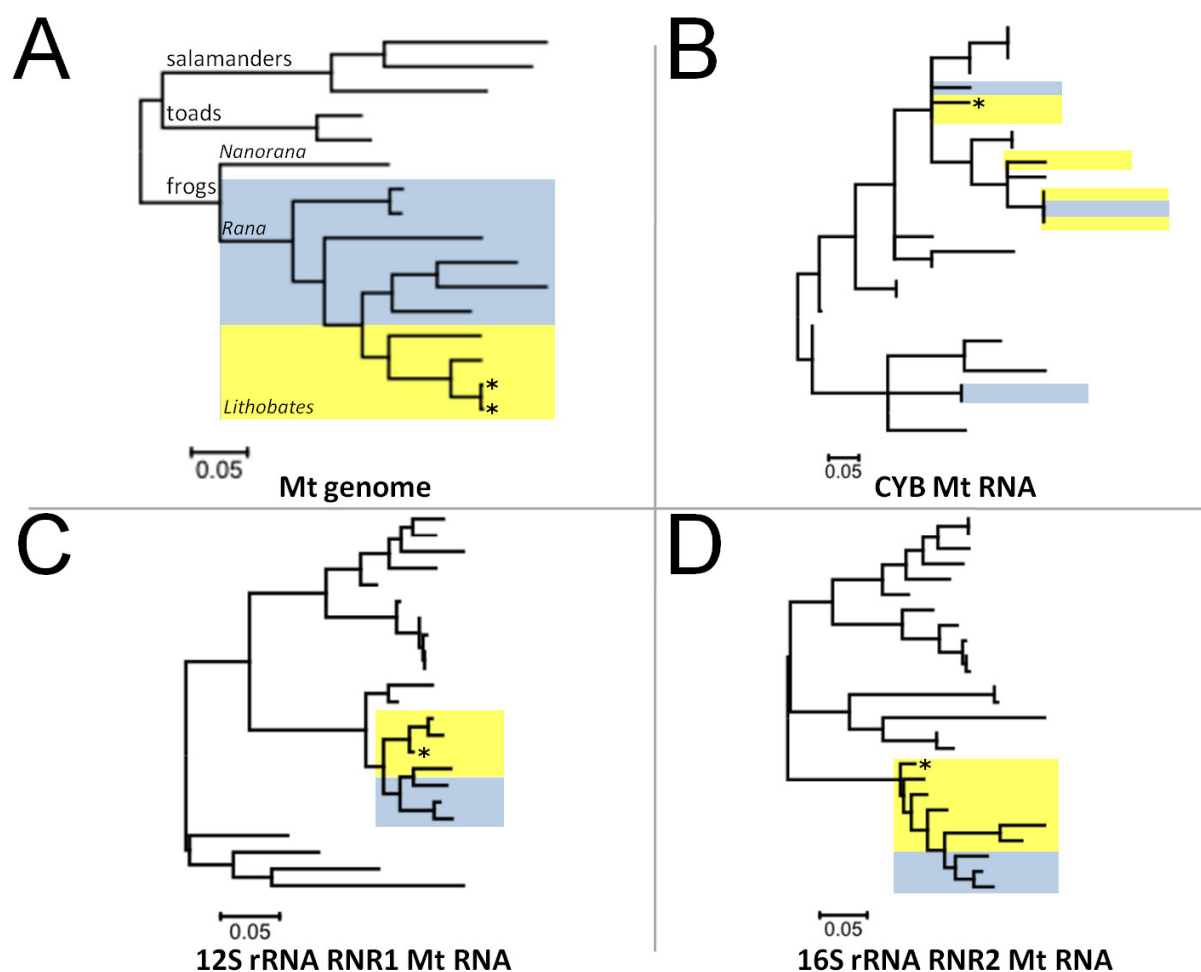
Figure 2. **Molecular phylogenetic analysis of amphibian Mitochondrial genomes and genes by Maximum Likelihood method.** The evolutionary history was inferred by using the Maximum Likelihood method based on the Tamura-Nei model (Tamura and Nei, 1993). The tree with the highest log likelihood is shown. Initial tree(s) for the heuristic search were obtained automatically by applying Neighbor-Join and BioNJ algorithms to a matrix of pairwise distances estimated using the Maximum Composite Likelihood (MCL) approach, and then selecting the topology with superior log likelihood value. The tree is drawn to scale, with branch lengths measured in the number of substitutions per site. The analysis involved A) complete mitochondrial (Mt) genome sequences of salamanders, toads and frogs (classified as *Rana* (blue highlight) or *Lithobates* (yellow highlights). Analysis of Mt genes B) CYB, C) RNR1, and D) RNR2 of selected frog species. Position of *R. catesbeiana* indicated by an asterisk. Evolutionary analyses were conducted in MEGA7 (Kumar, et al., 2016).

Tables

Table 1. Sequencing data for *R. catesbeiana* genome assembly

Library protocol	Read length (bp)	Sequencing platform	Nominal fragment length (bp)	# Libraries	# Reads (M)	Fold coverage
PET	150	HiSeq 2000	600	4	1187	30
PET	250	HiSeq 2500	550	8	736	31
PET	500	MiSeq	600	8 (same)	66	5
MPET	100	HiSeq 2000	9000-13000	4	262	5
SLR	N/A	HiSeq 2000	0.5 - 14000	1	0.6	0.5

Table 2. Assembly statistics for sequences 500 bp or more in length

	Unitig	Contig	Scaffold
Number ≥ 500 bp	2,737,303	2,191,947	1,548,590
Number ≥ N50	420,964	295,271	30,262
Number ≥ NG50	438,623	300,168	22,767
N80 (bp)	1,252	1,862	2,934
N50 (bp)	3,620	5,302	44,121
NG50 (bp)	3,509	5,239	57,718
N20 (bp)	8,198	11,740	155,955
Max (bp)	68,999	90,443	1,375,273
Reconstruction (Gbp)	5.715	5.787	5.842

Table 3. ABySS-Bloom sequence identity calculations between various draft genome assemblies*.

		Estimated time since divergence (MYA)		
		R. catesbeiana	*N. parkeri*	*X. tropicalis*
Estimated identity (%)	*R. catesbeiana*		89.0	208.6
	N. parkeri	$86.01 \pm 3.32 \times 10^{-4}$		208.6
	X. tropicalis	$79.16 \pm 3.42 \times 10^{-3}$	$77.92 \pm 2.51 \times 10^{-3}$	

*k=25, Sequences ≥ 500 bp

Supplemental Material

Supplemental Methods

Construction of a composite reference transcriptome (Bullfrog Annotation Resource for the Transcriptome; BART)

Transcriptome assemblies were generated from 32 *R. catesbeiana* tadpole samples (representing 5 tissues under several different chemical and temperature exposure conditions) using Trans-ABySS (Robertson, et al., 2010) (see Supplemental Table 2). The transcripts from each independent assembly were aligned using the BLAST-like Alignment Tool (Kent, 2002) or parallelized BLAT (pblat; icebert.github.io/pblat/) to identify highly similar sequences, where only the longest example of each set of similar sequences was retained. This process produced 794,291 transcripts 500 bp or longer, collected and termed the Bullfrog Annotation Resource for the Transcriptome (BART; available under NCBI BioProject PRJNA286013). Further, we report 1,341,707 transcripts between 200 and 499 bp long (termed BART Jr., and available at the BCGSC ftp: ftp://ftp.bcgsc.ca/supplementary/bullfrog).

Targeted gene assembly with Kollector

Kollector is an alignment-free targeted assembly pipeline that uses thousands of transcript sequences concurrently to inform the localized assembly of corresponding gene loci (Kucuk, et al., *submitted*). Kollector scans WGSS data to recruit reads that have sequence similarity to input transcripts or previously recruited reads, which are then assembled with ABySS. This greedy approach enables resolution of intronic regions for the assembly of complete genes.

39

To provide long-distance information to aid in scaffolding, we used Kollector to reconstruct the gene loci of the transcripts contained in the BART reference transcriptome. The BART transcripts were randomly divided into 80 bins of approximately 10,000 transcripts each, and Kollector run on each bin in parallel. To evaluate success of the targeted gene assemblies (TGA), the input transcripts were aligned to the Kollector-assembled sequences with BLASTn (Camacho, et al.), and those transcripts that aligned with 90% sequence identity and 90% query coverage were considered to have had their corresponding gene successfully reconstructed. Transcripts that did not meet these criteria were re-binned and re-tried in the next iteration with parameters tuned for higher sensitivity. This is achieved by lowering the r parameter (number of nucleotide matches required for recruiting a read) and the value of k used in the assembly step. After 5 Kollector iterations, 78% of BART transcripts were successfully assembled according to our criteria.

TH experiment

We sequenced transcriptomes from the back skin of three individual *R. catesbeiana* tadpoles that were injected with 10 pmol/g body weight of T_3 (Sigma-Aldrich Canada Ltd.) prepared in dilute NaOH (ACP Chemicals Inc.) and sacrificed 48 h post-injection. A matched group of vehicle only-injected tadpoles consisted of an additional group of 3 individual animals. Details of the exposures and evidence of tissue responsiveness to T_3 treatment using qPCR of these animals can be found in Maher *et al.* (2016). These samples were also used by Maher *et al.* (2016), but within the context of a separate study with distinct analyses focused solely on targeted qPCR of select mRNA transcripts.

Single-stranded RNA-seq libraries were generated from these six samples individually using Illumina HiSeq 2500 paired-end sequencing platform (San Diego, CA, USA) and 100 base pair (bp) paired end sequencing protocol following manufacturer's instructions. Information on the six read libraries is shown in Supplemental Table 4.

qPCR analysis of transcript abundance

Transcript abundance of three select transcripts encoding proteins involved in RNA/DNA processing was determined using methods and conditions published previously (Maher, et al., 2016). The primer sequences, annealing temperatures, and amplicon sizes are shown in Supplemental Table 9.

lncRNA detection

The workflow used to detect candidate lncRNAs is summarized in Supplemental Figure 2. First, open reading frames (ORFs) were predicted using TransDecoder v3.0.0 (transdecoder.github.io) with the default parameters, and contigs with complete or partial predicted ORFs were excluded. We also performed 3-frame *in silico* translations of the contigs to evaluate the validity of any potential encoded peptides via comparison to the Pfam curated database of peptide motifs (Finn, et al., 2014) using HMMScan v3.1b2 from the HMMER package (Finn, et al., 2015). Furthermore, we did a six-frame translation of our nucleotide sequences, and queried them against Uniref90 (Suzek, et al., 2015) and NCBI's RefSeq databases using the BLASTx (Camacho, et al., 2009) program from NCBI's BLAST+ (v2.4.0) software package. We discarded all contigs that returned a hit to any sequence in these databases at e-value $< 10^{-5}$. We constructed a comprehensive amphibian transcriptome shotgun assembly database (CATSA) by

downloading and combining nucleotide sequences for 16 amphibian species (Supplemental Table 4) from the NCBI- Genbank-Transcriptome Shotgun Assembly Sequence (TSA) database (Clark, et al., 2016). We interrogated our putative lncRNA contig set against this CATSA database for homologs that could add confidence to our set. We also did a similarity search against lncRNA sequences present in lncRNADB (Quek, et al., 2015) and LNCipedia (Volders, et al., 2015), which are databases of previously reported lncRNAs.

We assessed the coding potential of our contigs with Coding Potential Calculator (CPC) v0.9-r2 (Kong, et al., 2007), and filtered out any contig that returned a positive CPC score of greater than 1.

Supplemental Tables

Supplemental Table 1. Scaffolding the North American bullfrog genome with long-range distance information. TGA = targeted gene assembly; WGA = whole genome assembly.

Methodology	Data Source	Number of merges	NG50 (bp)	CEGMA Complete	CEGMA Complete + Partial
ABySS v1.9.0 k160	MPET (7kbp)	NA	23,361	81	190
RAILS v0.1	SLR (Moleculo) Kollector TGA	56,784	30,085	81	194
ABySS - longscaffolding v1.9.0	BART	NA	33,847	82	197
LINKS v1.7 x10	SLR (Moleculo)	29,178	34,492	83	197
LINKS v1.7	MPET (7 kbp)	108,578	50,123	93	199
LINKS v1.7 x7	Kollector TGA and k128 WGA	77,885	58,021	102	211

Supplemental Table 2. *R. catesbeiana* RNA-Seq data. Reads are available under NCBI

BioProject PRJNA286013. DE = read sets used for the differential gene expression

experiment; BART = read sets assembled with Trans-ABySS to construct BART.

References: (1) = Hammond, et al, 2015; (2) The present study.

Tissue	Chemical Condition	Sequencing Platform	Read Length (bp)	Read Pairs (M)	Utilization	Reference
Back Skin	dilute NaOH	HiSeq2000	75	139	BART	(1)
Back Skin	dilute NaOH	HiSeq2000	75	90	BART	(1)
Back Skin	dilute NaOH	HiSeq2500	100	135	DE, BART	(2)
Back Skin	dilute NaOH	HiSeq2500	100	178	DE, BART	(2)
Back Skin	dilute NaOH	HiSeq2500	100	156	DE, BART	(2)
Back Skin	10 nM T_3	HiSeq2000	75	121	BART	(1)
Back Skin	10 nM T_3	HiSeq2000	75	136	BART	(1)
Back Skin	10 nM T_3	HiSeq2500	100	158	DE, BART	(2)
Back Skin	10 nM T_3	HiSeq2500	100	141	DE, BART	(2)
Back Skin	10 nM T_3	HiSeq2500	100	161	DE, BART	(2)
Tail Fin	dilute NaOH	HiSeq2000	75	96	BART	(1)
Tail Fin	dilute NaOH	HiSeq2000	75	101	BART	(1)
Tail Fin	10 nM T_3	HiSeq2000	75	193	BART	(1)
Tail Fin	10 nM T_3	HiSeq2000	75	122	BART	(1)
Lung	dilute NaOH	HiSeq2000	75	108	BART	(1)
Lung	dilute NaOH	HiSeq2000	75	114	BART	(1)
Lung	10 nM T_3	HiSeq2000	75	125	BART	(1)
Lung	10 nM T_3	HiSeq2000	75	115	BART	(1)
Brain	dilute NaOH	HiSeq2000	75	110	BART	(1)
Brain	dilute NaOH	HiSeq2000	75	100	BART	(1)
Brain	dilute NaOH	HiSeq2000	75	98	BART	(1)
Brain	10 nM T_3	HiSeq2000	75	116	BART	(1)
Brain	10 nM T_3	HiSeq2000	75	101	BART	(1)
Brain	10 nM T_3	HiSeq2000	75	126	BART	(1)
Olfactory Bulb	solvent	MiSeq	100	9	BART	Unpublished
Olfactory Bulb	solvent	MiSeq	100	14	BART	Unpublished
Olfactory Bulb	solvent	MiSeq	100	8	BART	Unpublished
Olfactory Bulb	solvent	MiSeq	100	8	BART	Unpublished
Olfactory Bulb	Chemical Cocktail	MiSeq	100	12	BART	Unpublished
Olfactory Bulb	Chemical Cocktail	MiSeq	100	11	BART	Unpublished
Olfactory Bulb	Chemical Cocktail	MiSeq	100	8	BART	Unpublished
Olfactory Bulb	Chemical Cocktail	MiSeq	100	9	BART	Unpublished

44

Supplemental Table 3. DNA poly-A hexamer motifs considered for detection of cleavage site. Observed frequency of usage in *H. sapiens* noted for reference.

DNA hexamer	Usage frequency (*H. sapiens,* %)*
AATAAA	52.0%
ATTAAA	14.9%
TATAAA	3.2%
AGTAAA	2.7%
AATATA	1.7%
CATAAA	1.3%
GATAAA	1.3%
AATACA	1.2%
TTTAAA	1.2%
AAGAAA	1.1%
AAAAAG	0.8%
AATGAA	0.8%
AATAGA	0.7%
ACTAAA	0.6%
AAAACA	0.5%
GGGGCT	0.3%

* (Beaudoing, et al., 2000)

Supplemental Table 4. Amphibian species included in the CATSA database

Species or genus	TSA size (MB)
Ambystoma mexicanum	4.2
Bufotes viridis	45
Hynobius chinensis	97
Hynobius retardus	445
Leptobrachium boringii	45
Megophrys	45
Microhyla fissipes	85
Odorrana margaretae	41
Pelophylax nigromaculatus	47
Polypedates megacephalus	53
Pseudacris regilla	36
Rana clamitans	37
Rana pipiens	886
Rhacophorus dennysi	53
Rhacophorus omeimontis	39
Tylototriton wenxianensis	87

Supplemental Table 5. Complete mitochondrial genome sequences used in conjunction with our assembled *R. catesbeiana* mitochondrial genome sequence in the phylogenetic analysis

Species	GenBank Accession
A. mexicanum	AY659991.1
B. japonicas	NC_009886.1
B. tibetanus	NC_020048.1
N. parkeri	NC_026789.1
R. catesbeiana	AB761267.1
R. chosenica	NC_016059.1
R. draytonii	NC_028296.1
R. huanrensis	NC_028521.1
R. ishikawae	NC_015305.1
R. kunyuensis	NC_024548.1
R. nigromaculata	NC_002805.1
R. okaloosae	NC_028283.1
R. sibiricus	AJ419960.1
R. sylvatica	NC_027236.1
T. verrucosus	NC_017871.1

Supplemental Table 6. Mitochondrial genes used in phylogenetic analysis

Species	GenBank Accession		
	CYB	RNR1	RNR2
A. cognatus	x	x	DQ158444
A. crepitans	EF988143	AY843559	AY843559
A. fowleri	x	DQ158451	DQ158451
A. gracile	AY691729	x	x
A. macrodactylum	JX650148	x	x
A. montanus	DQ087517	x	AY236830
A. truei	AF277330	AJ871087	AJ871087
B. americanus	AB159264	AY680211	AY680205
B. baxteri	x	AY680207	AY680207
B. boreas	EU938403	EF531994	HM563856
B. cognatus	L10968	EF532241	x
H. chrysoscelis	AY830956	x	x
H. versicolor	AY830957	AY843682	AY843682
P. crucifer	KJ536191	AY843735	AY843735
P. maculata	KJ536217	x	KM669659
P. regilla	KJ536196	AY819376	AY291112
P. triseriata	KJ536224	AY843738	AY843738
P. vehiculum	JF521651	x	x
R. aurora	EU552211	DQ019590	DQ019607
R. cascadae	EU708878	AY779197	AY779197
R. catesbeiana	NC022696	M57527	M57527
R. clamitans	AY083277	KM273857	AY779204
R. luteiventris	AY016649	AY016717	AY779194
R. palustris	x	JN227372	AY779228
R. pipiens	EU370724	EU370710	DQ347323
R. pretiosa	EU708873	x	x
R. septentrionales	AY083272	AY779200	AY779201
R. sylvatica	NC027236	NC027236	NC027236
S. bombifrons	JX564896	JX564896	JX564896
S. intermontana	AY236785	x	AY236819
T. granulosa	EU880333	EU880333	x
X. laevis	NC001573	NC001573	NC001573

Supplemental Table 7. Estimated proportion of repetitive DNA sequences in *R. catesbeiana* and select organisms.

Species	Approx. haploid genome size (Gbp)	Estimated interspersed repeat content (%)	Reference
R. catesbeiana	5.8	62	The present study
H. sapiens	3.1	56	Smit, et al., 2013
N. parkeri	2.3	47*	Sun, et al., 2015
X. tropicalis	1.5	43*	Sun, et al., 2015

* transposable elements, only

Supplemental Table 8. Comparison of relative fold abundance of select back skin transcripts significantly increased upon T3 exposure.

	Fold abundance relative to control	
Transcript	RNA-seq	qPCR
thrb	3.1±0.1	8.4±0.1*
RNA/DNA processing		
snrpa	5.2±0.2	11.1±2.2
rrp8	3.5±0.2	3.1±0.8
suv39h1	2.5±0.2	3.6±1.4

* From Maher et al., 2016

Supplemental Table 9. Targeted qPCR primer information

Gene transcript	Primer name	Primer sequence	Amplicon length (bp)	Annealing temperature (^{o}C)
snrpa	150110	TCCCAGAAGAGACAAACGAG	211	64
	150111	GCAGGCTACTTTTTGGCAA		
rrp8	150114	TGACTCTGCGTTCCCGTAT	254	64
	150115	AGCATCACCACAGCCAAA		
suv91	150116	AAATGCGGATTACTACTG	248	60
	150117	CTCCAAATGAGTTAGGGT		

Supplemental Figures
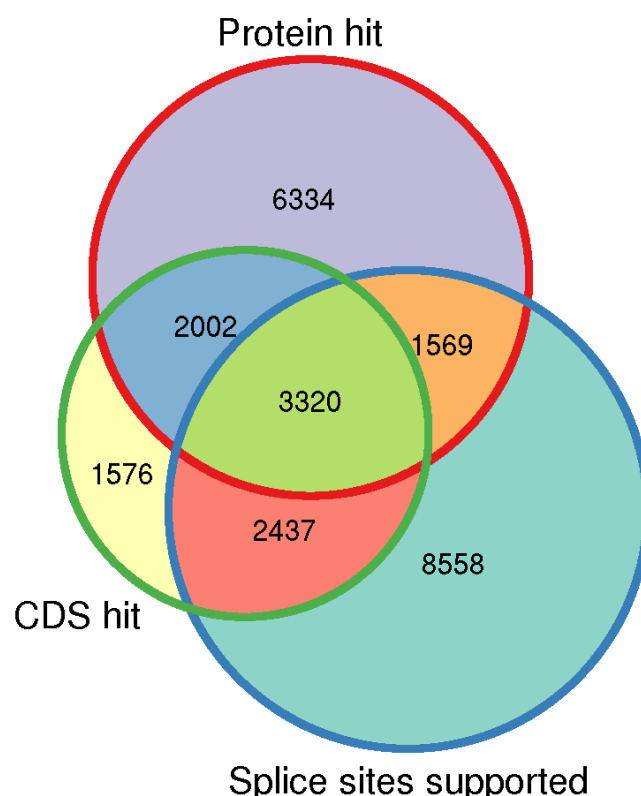
Supplemental Figure 1. **Selection criteria for the high confidence gene set.** MAKER2 predicted transcripts that had at least one splice site, all of which must be confirmed by an alignment to external transcript evidence ("Splice sites supported"), where the CDS of each transcript had a BLASTn alignment to a BART contig with at least 95% identity along 99% of its length (CDS hit), and where the protein sequence encoded by the CDS had a BLASTp alignment to a human or amphibian Swiss-Prot protein sequence with at least 50% identity along 90% of its length (Protein hit) were retained.
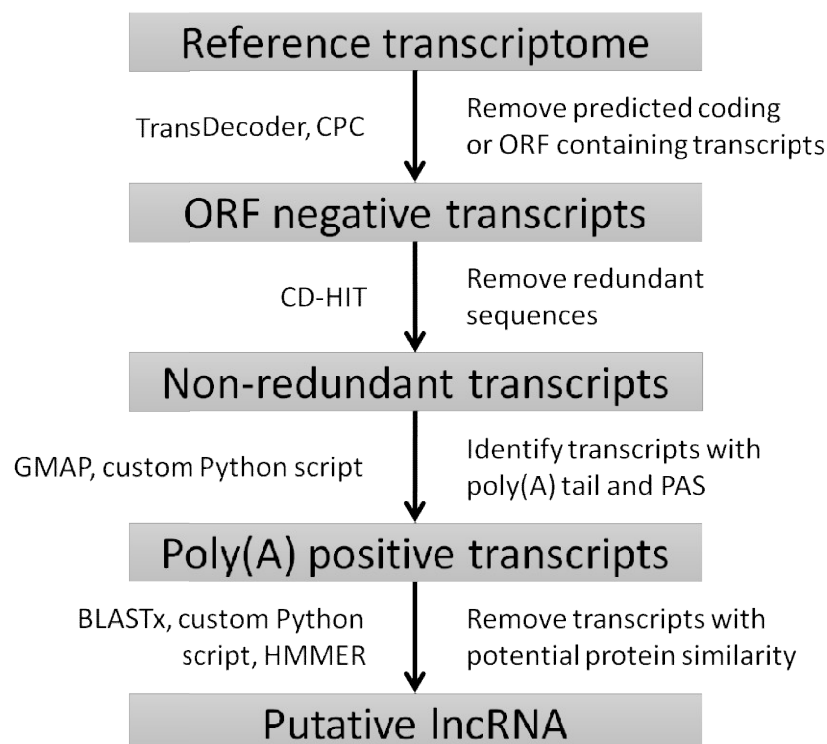
Supplemental Figure 2. **Workflow for detection of putative lncRNA transcripts.**

Supplemental Figure 3. **Enriched GO terms associated with genes differentially expressed in *R. catesbeiana* back skin following exposure to 10 nM T3 for 48 h.** RNA-seq reads were aligned to the genome with STAR, counts per high-confidence transcript determines with HTSeq, and differential expression in the T3 treated group relative to the vehicle control determined using DESeq2, where significance was at p < 0.05.
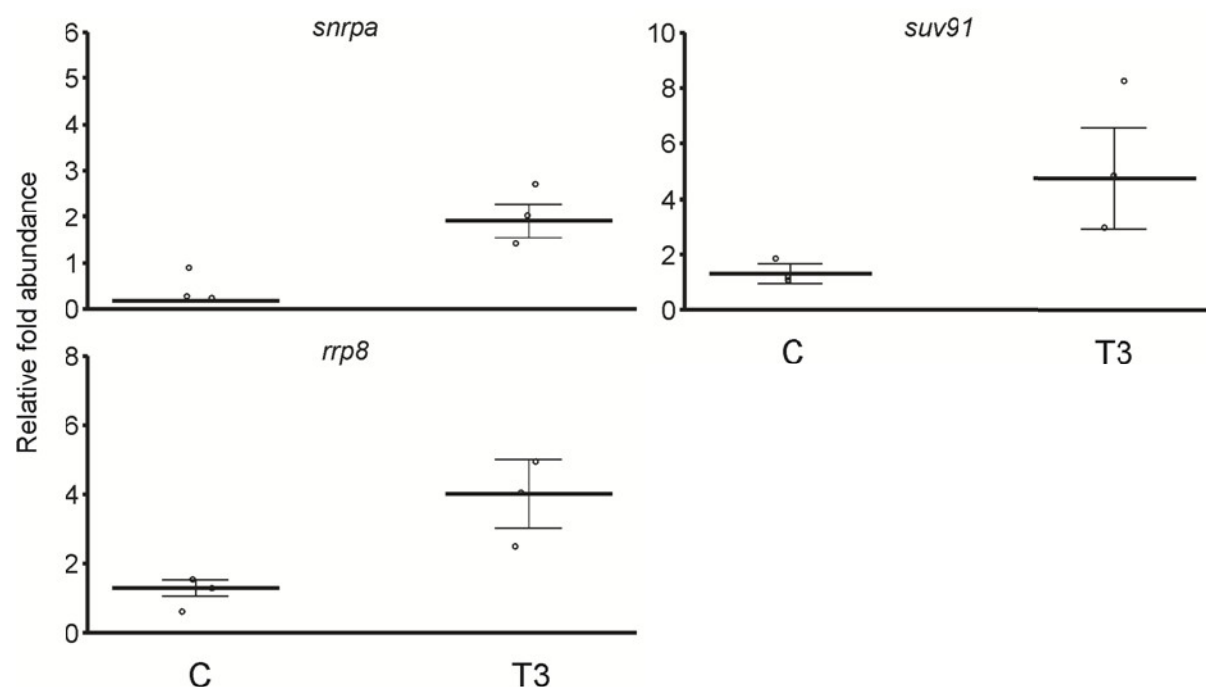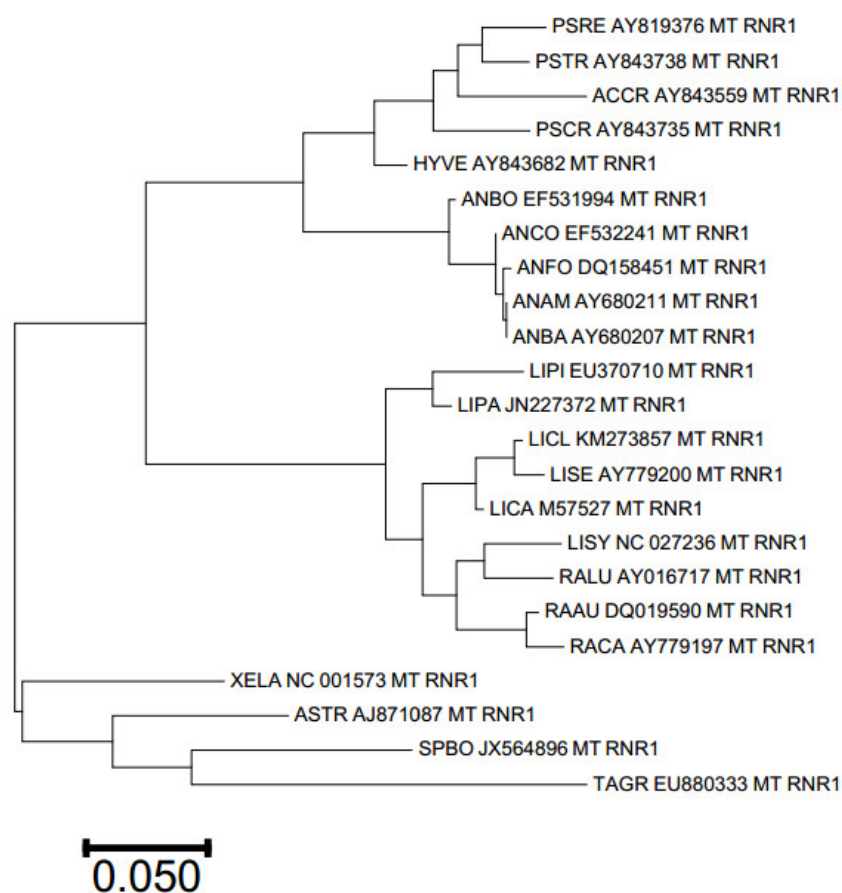
Supplemental Figure 4. **qPCR analysis of select transcripts encoding proteins involved in RNA/DNA processing in the back skin.** Premetamorphic tadpoles (n=3 per treatment) were injected with 10 pmol/g body weight of T3 or dilute sodium hydroxide solvent (C) and the back skin collected after 48 h for RNA isolation and qPCR analysis. The median fold abundance of transcripts encoding U1 small nuclear ribonucleoprotein A (*snrpa*), ribosomal RNA processing protein 8 (*rrp8*), and histone-lysine-N-methyltransferase *(suv91)* relative to the control is shown. Whiskers indicate the median absolute deviation, and the open circles denote the fold difference of individual animals. All transcripts were significantly different ($p < 0.05$).
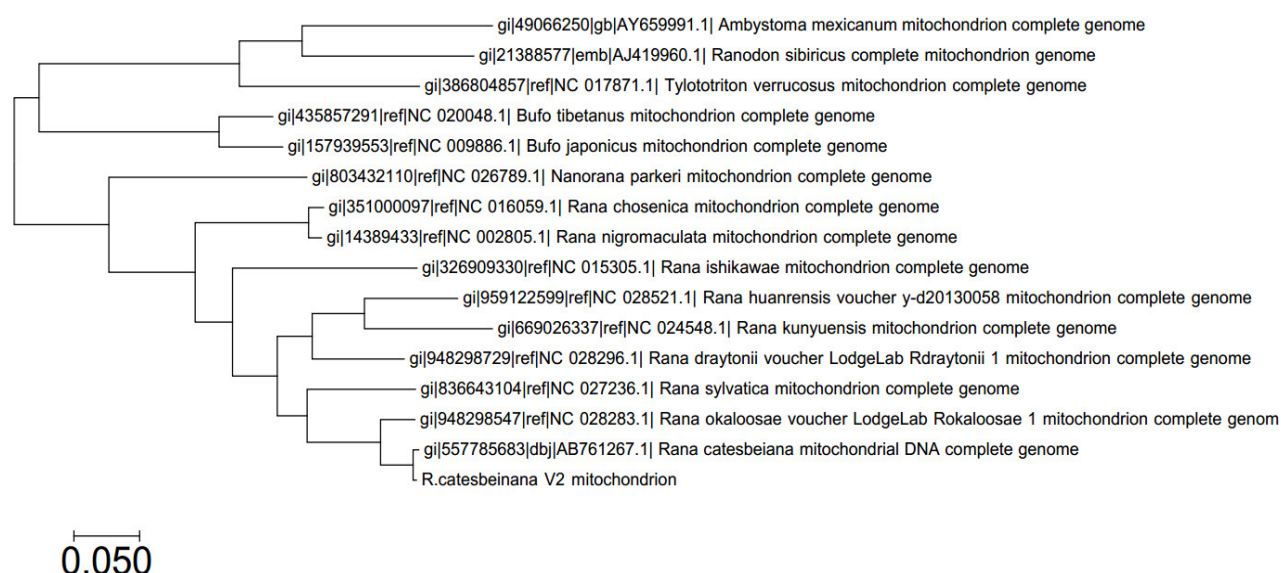
Supplemental Figure 5. **Molecular phylogenetic analysis of complete mitochondrial genomes of selected amphibians by Maximum Likelihood method.** The evolutionary history was inferred by using the Maximum Likelihood method based on the Tamura-Nei model (Tamura and Nei, 1993). The tree with the highest log likelihood (-91034.0605) is shown. Initial tree(s) for the heuristic search were obtained automatically by applying Neighbor-Join and BioNJ algorithms to a matrix of pairwise distances estimated using the Maximum Composite Likelihood (MCL) approach, and then selecting the topology with superior log likelihood value. The tree is drawn to scale, with branch lengths measured in the number of substitutions per site. The analysis involved 16 nucleotide sequences. All positions containing gaps and missing data were eliminated. There were a total of 10646 positions in the final dataset. Evolutionary analyses were conducted in MEGA7 (Kumar, et al., 2016).
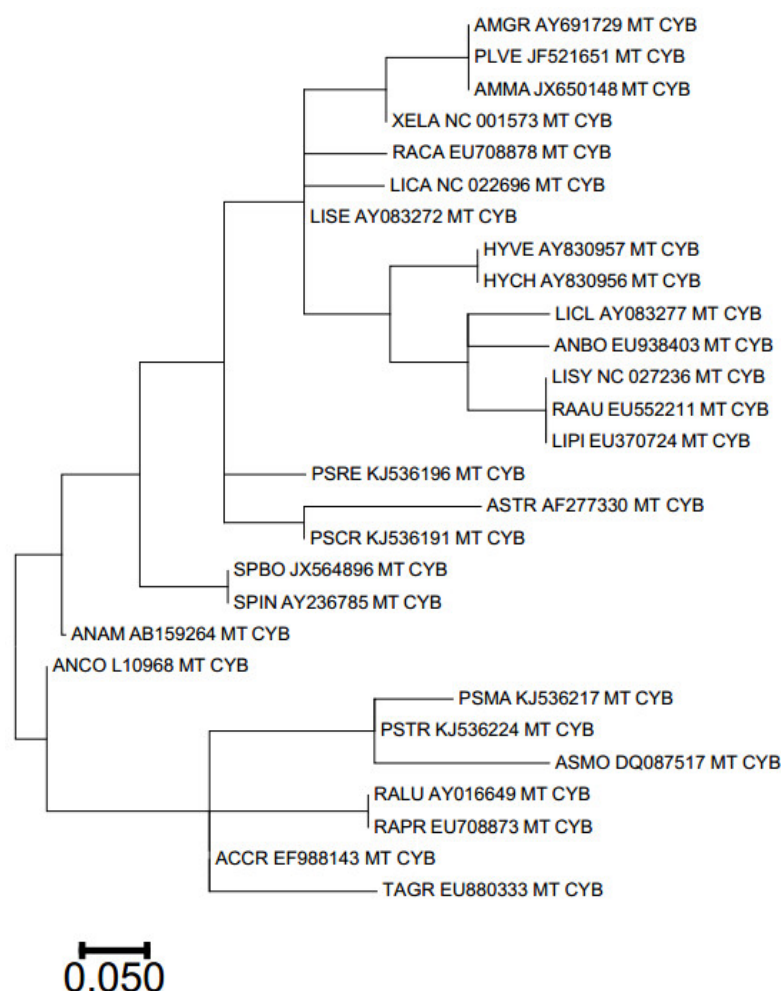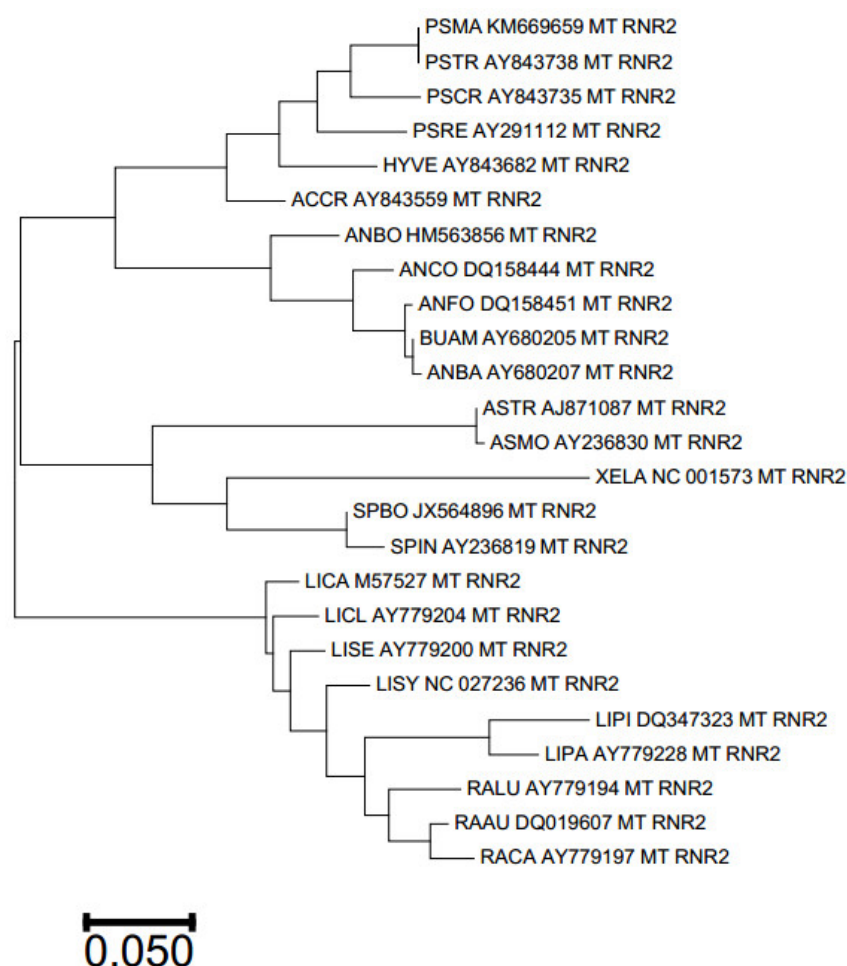
Supplemental Figure 6. **Molecular phylogenetic analysis of mitochondrial CYB (MT CYB) genes of selected amphibians by Maximum Likelihood method.** Sequences are annotated with the first two letters of the organisms' genus and species, respectively, followed by the NCBI GenBank accession number. See Supplemental Figure 5 legend for details of analysis and Supplemental Table 6 for additional information.

Supplemental Figure 7. **Molecular phylogenetic analysis of mitochondrial RNR1 (MT RNR1) genes of selected amphibians by Maximum Likelihood method.** Sequences are annotated with the first two letters of the organisms' genus and species, respectively, followed by the NCBI GenBank accession number. See Supplemental Figure 5 legend for details of analysis and Supplemental Table 6 for additional information.

Supplemental Figure 8. **Molecular phylogenetic analysis of mitochondrial RNR2 (MT RNR2) genes of selected amphibians by Maximum Likelihood method.** Sequences are annotated with the first two letters of the organisms' genus and species, respectively, followed by the NCBI GenBank accession number. See Supplemental Figure 5 legend for details of analysis and Supplemental Table 6 for additional information.